CHARACTERISTICS OF NANO-SELENIUM SYNTHESIZED BY Se(IV) ADSORPTION AND REDUCTION WITH ANOXYGENIC PHOTOSYNTHETIC BACTERIA

X. XIAO, C. ZHAO[*], S. YANG[*], S. GUO
*College of Chemical Engineering, Huaqiao University, Xiamen 361021, China
Mailing address: College of Chemical Engineering, Huaqiao University, No.668
Jimei Avenue, Xiamen, Fujian Province, 361021, China.*

One strain of resting cells of anoxygenic photosynthetic bacteria (*Rhodobacter sphaeroides* YL75), which is tolerant to Se(IV), was used in adsorption reduction of Se(IV) under anaerobic condition to produce red nano-selenium particles. The effects of different pH and NO_3^-, SO_4^{2-}, PO_4^{3-}, Cl^- anions on the adsorption reduction process were studied. And isothermal adsorption curve and adsorption kinetics curve of the strain YL75 were analyzed. The results showed that, the optimum pH of Se(IV) reduced by strain YL75 was 7, and the reduction rate of Se(IV) decreased with pH's shift to both sides. NO_3^-, SO_4^{2-}, Cl^- had minimum effect on reduction of Se(IV) by strain YL75, and competition between PO_4^{3-} and Se(IV) was found. It was presumed that strain YL75 transported Se(IV) to cell by phosphate ion channel. The adsorption of Se(IV) by strain YL75 was in accordance with Langmuir isotherm adsorption model (R^2 = 0.9505), indicating that adsorption of Se(IV) by strain YL75 was a single monolayer adsorption, and the mutual interference between two adjacent Se(IV) was negligible. The adsorptive capacity of strain YL75 for Se(IV) reached the equilibrium at 200 min, and its adsorption model accorded with pseudo-first-order kinetic model (R^2 = 0.9965), indicating that adsorption process of Se(IV) by strain YL75 was controlled by diffusion step, which concerned Se(IV) concentration in adsorption system solution. The strain YL75 was effective in removing Se(IV) in water, an environmentally friendly adsorption reducing agent.

1. Introduction

In recent years, with the rapid development of textile printing and electronic industry, selenium compounds have been increasingly concerned and widely used. Meanwhile, industrial waste water containing selenite and selenate gradually increased, which could cause serious pollution after entry into the water body and release to the environment without treatment. There are many microorganisms in nature, such as Azospirillum brasilens [1], Burkholderia fungorum [2], Pseudomonas fluorescens [3], Citrobacter fruendii strain KP6 [4], native Enterobacter sp. strain [5], Pantoea agglomerans strain UC-32 [6] etc. which have the ability to reduce oxidized selenium into selenium nanoparticles. The produced red selenium is easy to be recovered with less toxicity, which can be effectively used for treatment of wastewater containing oxidized selenium with good environmental friendliness. Compared with inorganic selenium and organic

---

*Corresponding author: email: chungui@hqu.edu.cn

selenium, red nano-selenium is characterized by low toxicity and high biological activity, which has relatively large application value in animal production, medicine and health care products [7-10]. Therefore, acquisition of red nano-selenium with environmentally friendly biosynthesis has important research significance and practical value.

In earlier stage, our research group selected a strain of anoxygenic photosynthetic bacteria (*Rhodobacter sphaeroides* YL75) with strong tolerance to Se(IV). In this study, the interference of living cell culture system to the experimental results was excluded. With resting cells of strain YL75 as research objects, its capacity in adsorption reduction of Se(IV) and generation of red selenium under anaerobic condition was further investigated. The influence of different conditions on adsorption reduction process was also studied. The isothermal adsorption curve and adsorption kinetic curve of strain YL75 resting cells versus Se(IV) were analyzed, with an aim to providing a reference for microbial remediation and control of environmental selenium pollution.

2. Materials and methods

2.1 Materials
2.1.1 Stain
Rhodobacter sphaeroides YL75 strain was isolated, identified and preserved from Lab of Huaqiao University.
2.1.2 Culture medium
The improved Ormerod[11] culture medium, 6.0 g/L sodium malate and 0.5 g/L ammonium sulfate in the formula are changed to 2.46 g/L sodium acetate and 1.0 g/L sodium glutamate, respectively.
2.1.3 Major instruments and reagents
UV-3200PCS UV-visible spectrophotometer, MAPADA. 5417R desktop high-speed centrifuge, Eppendorf. Delta 320 pH meter, METTLER-TOL Instruments (Shanghai) Co., Ltd. BX51 microscope, Olympus. ZRX-300E intelligent artificial climate incubator, Hangzhou Qianjiang Instruments & Equipment Co., Ltd. THZ-82 vapor-bathing constant temperature vibrator, Jiangsu Jinwei Experimental Instrument Factory. Energy Dispersive X - ray Spectrometer, Jiangsu Skyray Instrument Co., Ltd. Sodium chloride, methylene blue and Triton X-100, etc. are domestic analytical reagent.

2.2 Methods
2.2.1 Determination of bacterial suspension concentration (OD_{660})
The optical density (OD_{660}) at 660 nm indicates bacterial suspension concentration. OD_{660} was measured on a spectrophotometer using a cuvette with a path length of 1 cm. The mass concentration (g/L) of the bacterial suspension was calculated by the relationship between cell wet weight and OD_{660}.
2.2.2 Preparation of resting cells
The inoculum size was 5% (v/v). After inoculation, the culture bottle was filled with sterile culture medium and cultured in anaerobic culture. The culture conditions were 28 ℃, 3000 lx. After 96 h culture, centrifuge 8 min at 8 000 x g to collect strain to be washed 3 times with sterile physiological saline to prepare bacterial suspension with OD_{660} at 2.5. After 48 h static incubation at 28 ℃, resting cell suspension was obtained. Accurate measurement is needed in usage.
2.2.3 Preparation of Se(IV) stock solution
The 2.63 g of Na$_2$SeO$_3$ was accurately weighed and dissolved to a volume of 100 mL.

Se(IV) stock solution at a concentration of 0.1 mol / L was prepared and stored at 4 °C in the dark.

2.2.4 Determination of Se(IV)

Se(Ⅳ) content was determined by the color-spectrophotometric methodof Se(Ⅳ)-iodide-methylene blue-Triton X-100 association complex system[12].

2.2.5 Nano-selenium synthesized by strain YL75

YL75 resting cell suspension and Se(IV) stock solution at 25 °C constant temperature were accurately weighted, to be added in 250 mL Erlenmeyer flask. After adding 50 mL pH 7.0 sterile saline solution, incubate 48 h in vapor-bathing thermostatic shaker at 25 ℃.

2.2.6 Effect of different pH and anion on Se(IV) reduction rate

Add appropriate amount of YL75 resting cell suspension to a certain amount of Se(IV) stock solution, to be cultured 48 h in shaker respectively at pH of 4,6,7,8,9,10, followed by determination of Se(IV) reduction rate. Under the optimal pH, add Cl^-, PO_4^{3-}, SO_4^{2-}, NO_3^-, then culture for 48 h in shaker, followed by determination of Se(IV) reduction rate. Computational formula of reduction rate (r) of Se(IV):

$$r \% = （c_0 - c_t） / c_0 \cdot 100\% \tag{1}$$

In the formula, c_0 and c_t represent the initial concentration of Se(IV) and the concentration (mg/L) at the time of measurement, respectively.

2.2.7 Determination of adsorption of Se (IV) by strain YL75

Appropriate amount of YL75 resting cell suspension was weighted, to be added with Se(IV)

solution of different concentrations. The reaction system was determined to be 1.5 mL. The reaction system was placed in a thermostatic shaker at 25 ℃. After Se(IV) was adsorbed by the cells for a period of time, the supernatant was centrifuged to determine adsorption of Se(IV) by cells.

The adsorption capacity of Se(IV) by cell is calculated by the formula:

$$Q = （c_0 - c_t） \cdot V/W \tag{2}$$

Wherein, c_0 and c_t represent the initial concentration of Se(IV) and the concentration (mg/L) at the time of measurement, respectively; Q is the adsorption reduction amount (mg/g) of Se(IV) by t h somatic cell; V is volume (L) of action system; W is the weight (g) of wet cell.

2.2.8 Isothermal adsorption model

The thermodynamic models of Langmuir [13] and Freundlich [14] were used to describe the isothermal adsorption process of Se(IV) by YL75 resting cells.

$$\text{The Langmuir model equation is: } C_e/Q_e = 1/(K_L Q_m) + C_e/Q_m \tag{3}$$
$$\text{The Freundlich model equation is } \ln Q_e = \ln K_F + 1/n \ln C_e \tag{4}$$

In the formula, Q_e and Q_m represent the adsorption capacity of Se(IV) by cell and theoretical maximum monolayer adsorption capacity respectively. C_e and K_L respectively indicate Se(IV) concentration and adsorption equilibrium constant in the solution at adsorption equilibrium, K_F and n are respectively adsorption coefficient and adsorption constant of Freundlich model.

2.2.9 Adsorption kinetic model

The adsorption kinetics process of Se(IV) by YL75 resting cells was described by 5 kinetic models of Elovich [15], double constant [16], pseudo-first order [17], pseudo-second

order [18] and intraparticle diffusion [19].

Elovich model equation is: $Q_t = A + B\ln t$ (5)

The double constant model equation is: $\ln Q_t = A + B\ln t$ (6)

The pseudo-first-order model equation is: $\ln(Q_e - Q_t) = \ln Q_e - Kt$ (7)

The pseudo-second-order model equation is: $t/Q_t = 1/2KQ_e^2 + t/Q_e$ (8)

The intraparticle diffusion model equation is: $Q_t = A + Kt^{0.5}$ (9)

Wherein, Q_t and Q_e respectively represent the adsorption amount and saturated adsorption amount at time t, t is the adsorption time, and K is the adsorption rate constant.

2.2.10 Identification of reduction product of nano-selenium particles

After 48 h of reaction, selenium nanoparticles were released from micro-organisms by high-temperature sterilization [20], to be cooled to room temperature and centrifuged at 3000 r·min^{-1} for 5 min. The red product was collected and washed with ultrapure water three times. The resulting product was dried at 80 ℃ and then characterized and identified by EDX (Energy Dispersive X-Ray Spectroscopy).

3. Results and discussion

3.1 Property of reduction of Se(IV) by strain YL75

The 0.1 m M Se (IV) stock solution was added to YL75 resting cell suspension at 25 ℃ and the color of the solution turned red after 48 h incubation at 25℃ in vapor-bathing thermostatic shaker. Microscopic examination showed that obvious granular material was observed in resting cells of YL75 in the above reaction system, but no particulate matter was observed in blank control YL75 resting cell suspension without Se (IV) stock solution, and the solution color did not change (see Figure 1-a, Figure 1-b). Jiang et al [21] reported reduction of sodium selenite by *pseudomonas* MBR, proved that the red product was elemental selenium. Therefore, it is speculated that strain YL75 also has the ability to reduce Se(IV). After incubation at 25 ℃ for 60 h in vapor-bathing thermostatic shaker, extracellular selenium particles were observed in the resting cells of YL75. It was deduced that selenium particles produced by adsorption reduction of Se(IV) were exhausted by strain YL75 (See Figure 1-c).
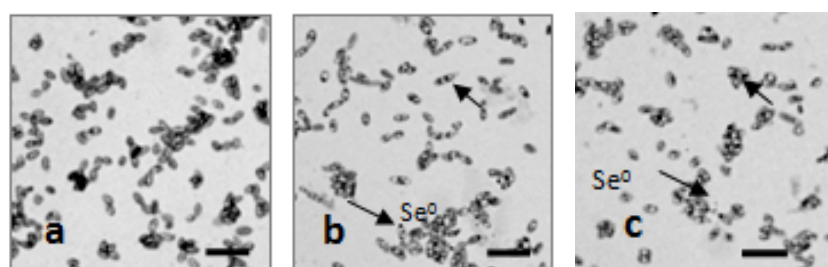

Fig. 1. Microscopic examination of Se (IV) reduced by YL75 strain (bar: 5 μm) a. blank control without Se (IV) stock solution, b. reaction system added with Se(IV) stock solution; c. after 60 h reaction, extracellular selenium particles are visible)

3.2 Effect of different pH, anion on Se(IV) reduction rate

3.2.1 Effect of different pH on Se(IV)reduction rate

pH can influence reduction capacity of Se(IV) by affecting activity of the enzyme. In order to obtain the optimum pH for reduction of Se(IV) by strain YL75, the reduction rate of

Se(IV) under different pH was studied. The formation of red reduction products was observed in the range of pH 4-10. The experimental results are shown in Figure 2. It can be seen from Figure 2 that, reduction rate of Se(IV) by strain YL75 increases and then decreases in the inspected pH range. At pH 7, reduction rate of Se(IV) was the highest. The results indicated that both low pH and high pH could affect reduction rate of Se(IV) by strain YL75. It was speculated that, cell surface of strain YL75 was highly protonated at low pH, and could bind well with anion of selenite. At high pH, the surface of YL75 cell was negatively charged after hydroxyl adsorption layer formed or a very weak acidic group mutually repelled by negatively charged selenite formed on the cell surface after ionization.
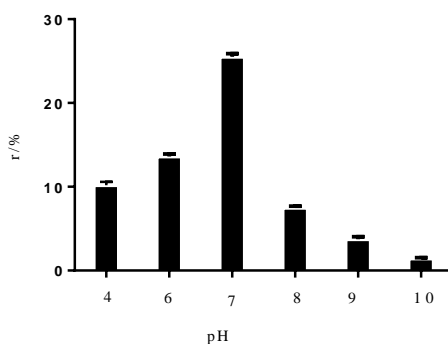

Fig. 2 Effect of pH on reduction of Se(IV) by strain YL75

3.2.2 Effect of different anions on Se(IV) reduction rate

SO_4^{2-}, NO_3^-, PO_4^{3-}, Cl^- are the more common anions in water and soil, and have a wider influence on microbial activity and biotransformation of other elements [22-24]. In this study, the effects of SO_4^{2-}, NO_3^-, PO_4^{3-}, Cl^- on reduction rate of Se(IV) were investigated. The results are shown in Figure 3. It can be seen from Figure 3 that, strain YL75 can reduce Se(IV) in different degrees under SO_4^{2-}, NO_3^-, PO_4^{3-}, Cl^-. Wherein, the reduction rate under PO_4^{3-} was the lowest. The reason may be that Se(IV) enters the cell through the phosphate ion channel on the cell membrane, but presence of PO_4^{3-} can compete with Se(IV), which may affect adsorption of Se(IV) into the cell membrane, and then reduction rate of Se(IV) by YL75 resting cells is affected.
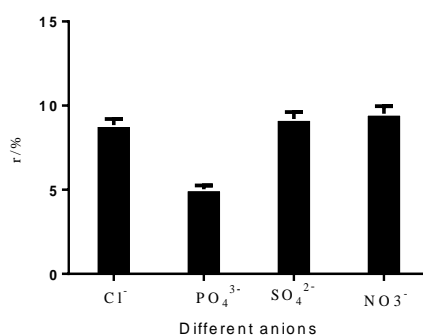

Fig. 3 Effect of anion on reduction of Se(IV) by strain YL75

3.3 Determination of Adsorption Isothermal curve of Se(IV) versus Strain YL75

The isothermal adsorption curve of Se(IV) versus strain YL75 at 25 ℃ is shown in Fig. 4. With the rise of initial concentration of Se(IV) in the reaction system, adsorption capacity

of YL75 gradually increased and reached saturation. When the concentration of Se(IV) reached 102 mg/L and 300 mg/L, adsorption capacity of YL75 reached to saturation, and the maximal adsorption capacity of YL75 for Se(IV) was 6.0 mg/g. The adsorption capacity of strain YL75 for Se(IV) was increased by 3 times as compared with that of control group with equal volume of sterile water. The results indicated that strain YL75 had a certain adsorption affinity to Se(IV), and could well adsorb Se(IV).
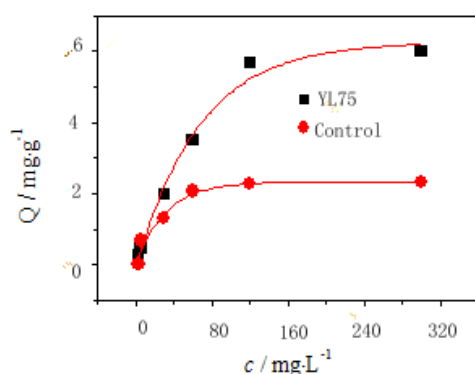

Fig. 4 Isothermal adsorption equilibrium curve of strain YL75 versus Se(IV)

3.4 Isothermal adsorption model analysis

Fig. 5 shows Langmuir and Freundlich models of adsorption of Se(IV) by strain YL75, which are obtained by C_e / Q_e vs C_e and $\ln Q_e$ vs $\ln C_e$ plotting of data in Figure 4 after linear fitting, respectively. The thermodynamic parameters of adsorption of Se(IV) by strain YL75 were obtained as shown in Table 1. As shown in Table 1, adsorption process of Se(IV) by strain YL75 is in good agreement with Langmuir isotherm model ($R^2 = 0.9505$), which indicates that adsorption process of Se(IV) by strain YL75 is monolayer adsorption and mutual interference of two adjacent Se(IV) in the adsorption process is negligible.
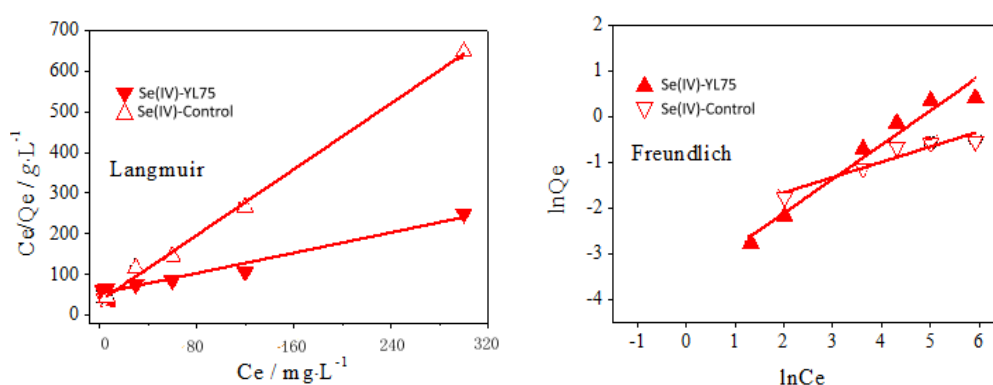

Fig. 5 Curves of Langmuir and Freundlich models for adsorption of Se(IV) by strain YL75

Table 1 Parameters of Langmuir and Freundlich models for adsorption process of Se(IV) by strain YL75

Model	Adsorbent	Equation	R^2
Langmuir	YL75	$C_e/Q_e=0.824C_e+53.176$	0.9505
	Control	$C_e/Q_e=4.152C_e+19.443$	0.9924
Freundlich	YL75	$\ln Q_e= 0.671\ln C_e\text{-}4.387$	0.7082
	Control	$\ln Q_e= 0.353\ln C_e\text{-}2.464$	0.8536

3.5 Adsorption kinetic analysis

The adsorption kinetics of YL75 versus Se(IV) is shown in Figure 6. At the initial stage of adsorption, the adsorption rate was very fast, which gradually decreased with the prolongation of time. The adsorption equilibrium was reached at about 200 min. The adsorption capacity of strain YL75 for Se(IV) did not change with prolongation of time. The relation curves of kinetic model were drawn by plotting of adsorption kinetic curve data with Q_t vs $\ln t$, $\ln Q_t$ vs $\ln t$, $\ln(Q_e\text{-}Q_t)$ vs t, t/Q_t vs t and Q_t vs $t^{0.5}$ respectively. The kinetic equation of Elovich, double constant, pseudo-first order, pseudo-second order and intraparticle diffusion and linear correlation coefficient (R^2) and corresponding kinetic parameters were obtained after linear fitting. The results are shown in Table 2. It can be seen from Table 2 that pseudo-first-order model fitting is the best ($R^2 = 0.9965$), indicating that adsorption process of Se(IV) by YL75 is controlled by diffusion step, which is related to Se(IV) concentration in the adsorption system solution.
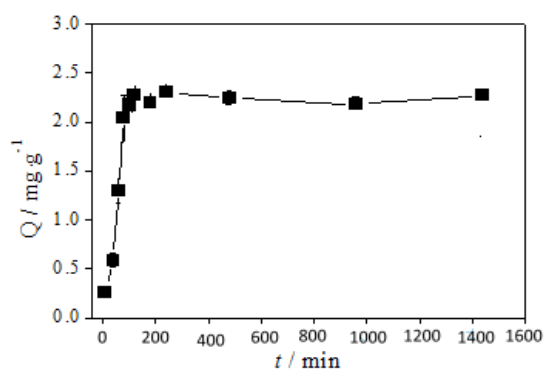

Fig. 6. Adsorption kinetic curve of YL75 versus Se(IV)

Table 2. Parameters of adsorption kinetic model of strain YL75 versus Se(IV)

Model	Equation	R^2
Elovich	$Q_t= 0.827 \ln t\text{-}1.536$	0.8932
Double constant	$\ln Q_t= 0.915 \ln t - 3.142$	0.8746
Pseudo-first-order	$\text{Ln}(Q_e\text{-}Q_t)= 2.846 +0.134t$	0.9965
Pseudo-second-order	$t/Q_t= 0.076\ t+25.762$	0.7714
Intraparticle diffusion	$Q_t= 0.562\ t^{\wedge}1/2\text{-}0.735$	0.8966

3.6 Identification of nano-selenium particles

In order to further confirm that the reduction product is nano-selenium particle, the reduction product was characterized by EDX, and the results are shown in Figure 7. It can be seen from Figure 7 that characteristic absorption peak of selenium can be observed at 11.2 keV, which indicates that the main component of the reduction product is selenium [25]. The signal of Cu appears in the graph, which may be derived from copper network, while C, P and O elements may be derived from extracellular secretions of the cells [26].
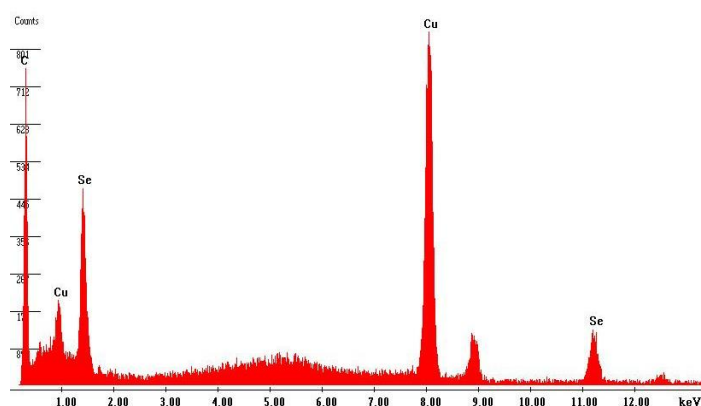

Fig. 7 EDX graph of nano-selenium particle of reduced product

4. Conclusion

This study demonstrated that a strain of anoxygenic photosynthetic bacteria, YL75, was able to reduce Se(IV) to red nano-selenium particles. pH is an important factor affecting reduction of Se(IV), and reduction rate of Se(IV) was the highest at pH 7. PO_4^{3-}, also a factor affecting reduction of Se(IV), competes with Se(IV) and inhibits reduction of Se(IV). The pseudo-first-order kinetic model can be used to describe adsorption kinetics process of strain YL75 versus Se(IV).

Fitting of Langmuir adsorption isotherm equation is better than that of Freundlich adsorption isotherm equation, indicating that adsorption of Se(IV) by strain YL75 is more inclined to monolayer adsorption. The transformation of selenium in nature is inseparable from action of microorganisms. The study of characteristics of biosynthesized selenium by strain YL75 is of great significance to biological selenium supplement, development and utilization of bio-selenium optical material, microbial remediation of selenium-contaminated environment. The strain YL75 can be used for treatment of wastewater containing oxidized selenium. With good environmental friendliness, it enjoys very broad application prospect.

References

[1] A. V. Tugarova, E. P. Vetchinkina, E. A. Loshchinina, A. M. Burov, V. E. Nikitina, A. A. Kamnev, Microbial Ecology, **68**(3), 1 (2014).

[2] N. S. Khoei, S. Lampis, E. Zonaro, K. Yrjälä, P. Bernardi, G. Vallini, New Biotechnology, **34**, 1 (2017).

[3] Nidhi Singh, Prasenjit Saha, Karthik Rajkumar, Jayanthi Abraham. International Journal of Nanoscience, **14**(4), 1550017 (2015).

[4] S. Samant, M. Naik, K. Parulekar, L. Charya, D. Vaigankar Selenium reducing *citrobacter fruendii* strain kp6 from mandovi estuary and its potential application in selenium nanoparticle synthesis. Proceedings of the National Academy of Sciences India, 1-8. (2016).

[5] N. Mollania, R. Tayebee, F. Narenji-Sani, Research on Chemical Intermediates, **42**(5), 4253 (2015).

[6] S. K. Torres, V. L. Campos, C. G. León, S. M. Rodríguez-Llamazares, S. M. Rojas, M. González, et al. Journal of Nanoparticle Research, **14**(11), 1 (2012).

[7] A. Bhattacharjee, A. Basu, J. Biswas, T. Sen, S. Bhattacharya, Chemoprotective and chemosensitizing properties of selenium nanoparticle (nano-se) during adjuvant therapy with cyclophosphamide in tumor-bearing mice. Molecular & Cellular Biochemistry, 1-21. (2016).

[8] A. Bhattacharjee, A. Basu, T. Sen, J. Biswas, S. Bhattacharya, Nano-se as a novel candidate in the management of oxidative stress related disorders and cancer. Nucleus, 1-9. (2016).

[9] S. A. Wadhwani, U. U. Shedbalkar, R. Singh, B. A. Chopade, Applied Microbiology and Biotechnology, **100**(6), 2555 (2016).

[10] K. Kalishwaralal, S. Jeyabharathi, K. Sundar, A. Muthukumaran, Medical Devices, and Artificial Organs, 44(2), 1 (2016).

[11] J. G. Ormerod, K. S. Ormerod, H. Gest, Archives of Biochemistry & Biophysics **94**(3), 449 (1961).

[12] R. Y. Li, Y. M. Li, J. H. Zhou, C. H. Zhang, Metallurgical Analysis, **29**(3), 45 (2009).

[13] F. T. Leighton International Journal for Numerical and Analytical Methods in Geomechanics, **39**(6), 594 (2015).

[14] Z. Maderova, E. Baldikova, K. Pospiskova, I. Safarik, M. Safarikova, International Journal of Environmental Science and Technology, **13**(7), 1653 (2016).

[15] O. Elijah, N. Joseph, Scientific Online Publishing, **1**(2), 133 (2014).

[16] E. Álvarez-Ayuso, A. García-Sánchez, X. Querol, Journal of Hazardous Materials, **142**(1–2), 191 (2007).

[17] Y. C. Wong, Y. S. Szeto, W. H. Cheung, G. Mckay, Journal of Applied Polymer Science, **92**(3), 1633 (2004).

[18] D. Robati Journal of Nanostructure in Chemistry, **3**(1), 1 (2013).

[19] F. C. Wu, R. L. Tseng, R. S. Juang, Chemical Engineering Journal, **153**(1-3), 1 (2009).

[20] P. J. Fesharaki, P. Nazari, M. Shakibaie, S. Rezaie, M. Banoee, M. Abdollahi, A. R. Shahverdi, Braz.j.microbiol, **41**(2), 461 (2010).

[21] S. Jiang, C. T. Ho, J. H. Lee, H. V. Duong, S. Han, H. G. Hur, Chemosphere, **87**(6), 621 (2012).

[22] J. Luster, A. Göttlein, B. Nowack, G. Sarret, Plant & Soil, **321**(1-2), 457 (2009).

214

[23] E. Adamek, W. Baran, J. Ziemiańska, A. Sobczak, Applied Catalysis B Environmental, **126**(9), 29 (2012).

[24] F. Trum, H. Titeux, J. Ranger, B. Delvaux, Annals of Forest Science, **68**(4), 837 (2011).

[25] M. Shakibaie, M. R. Khorramizadeh, M. A. Faramarzi, O. Sabzevari, A. R. Shahverdi, Biotechnology and Applied Biochemistry, **56**(1), 7 (2010).

[26] S. Dhanjal, S. S. Cameotra, Microbial Cell Factories, **9**(1), 52 (2010).